npg

ORIGINAL ARTICLE

Decreased *in vitro* mitochondrial function is associated with enhanced brain metabolism, blood flow, and memory in Surf1-deficient mice

Ai-Ling Lin[1,2,3,7], Daniel A Pulliam[2,3,7], Sathyaseelan S Deepa[2,3], Jonathan J Halloran[2,4], Stacy A Hussong[2,4], Raquel R Burbank[2,4], Andrew Bresnen[1], Yuhong Liu[2,3], Natalia Podlutskaya[2,3,4], Anuradha Soundararajan[1], Eric Muir[1], Timothy Q Duong[1,4], Alex F Bokov[2,3], Carlo Viscomi[5], Massimo Zeviani[5], Arlan G Richardson[2,3,6], Holly Van Remmen[2,3,6], Peter T Fox[1,4] and Veronica Galvan[2,4]

Recent studies have challenged the prevailing view that reduced mitochondrial function and increased oxidative stress are correlated with reduced longevity. Mice carrying a homozygous knockout (KO) of the *Surf1* gene showed a significant decrease in mitochondrial electron transport chain Complex IV activity, yet displayed increased lifespan and reduced brain damage after excitotoxic insults. In the present study, we examined brain metabolism, brain hemodynamics, and memory of Surf1 KO mice using *in vitro* measures of mitochondrial function, *in vivo* neuroimaging, and behavioral testing. We show that decreased respiration and increased generation of hydrogen peroxide in isolated Surf1 KO brain mitochondria are associated with increased brain glucose metabolism, cerebral blood flow, and lactate levels, and with enhanced memory in Surf1 KO mice. These metabolic and functional changes in Surf1 KO brains were accompanied by higher levels of hypoxia-inducible factor 1 alpha, and by increases in the activated form of cyclic AMP response element-binding factor, which is integral to memory formation. These findings suggest that Surf1 deficiency-induced metabolic alterations may have positive effects on brain function. Exploring the relationship between mitochondrial activity, oxidative stress, and brain function will enhance our understanding of cognitive aging and of age-related neurologic disorders.

INTRODUCTION

For the past four decades, reduced mitochondrial function has been regarded as one of the major factors promoting aging and age-related neurodegenerative disorders.[1] Mitochondrial dysfunction causes decreased energy (ATP) production, reduced oxygen consumption rate, and increased reactive oxygen species (ROS) generation. Reactive oxygen species are thought to cause oxidative stress, damage cellular structure, and ultimately lead to widespread cellular dysfunction and death. Preserved mitochondrial integrity, therefore, is generally presumed to be necessary for increased longevity as well as preserved brain functionality during aging.

Surprisingly, recent studies have suggested that decreased mitochondrial respiration and increased ROS generation are associated with extended lifespan in various organisms.[2–5]

The extension of lifespan in *C. elegans* by mitochondrial mutations has been shown to be dependent on hypoxia-inducible factor (HIF)-1 signaling.[3] Hypoxia-inducible factor are highly conserved transcription factors that are stabilized when oxygen decreases in the cellular environment,[6] or when the electron transport chain is inhibited.[3] Increased HIF-1 activates genes to promote survival during hypoxia. In *C. elegans*, HIF-1 is activated by elevated ROS production and is associated with increased longevity.[3] Hypoxia-inducible factor-1 forms a transcriptional complex with and can activate cAMP response element-binding (CREB) protein,[7] which has a key role in long-term memory and learning.[8] Thus, reduced mitochondrial respiration may extend lifespan and concomitantly enhance memory.

In mammals, a correlation between reduced mitochondrial function and extended longevity was recently observed in mice in which the *Surf1* gene contained a premature STOP mutation (Surf1 KO; *Surf1*^{−/−}). Surf1 participates in the efficient assembly and function of cytochrome C oxidase (COX; mitochondrial Complex IV), which is the terminal enzyme of the electron transport chain and is critical for ATP synthesis. In spite of showing reduced COX levels and activity (to 25% to 50% of control), median lifespan of Surf1 KO mice was increased by 21% compared with control mice.[9] Moreover, brains of Surf1 KO mice were shown

to be remarkably resistant to excitotoxic insults.[9] These observations suggest that Surf1 deficiency may have a positive impact on brain functionality as resistance to toxicity is expected to be associated with improved tissue function. This hypothesis, as well as indices of brain integrity and function such as metabolism and hemodynamics in Surf1 KO mice, remained largely unexplored. The purpose of this study was to determine the relationship between among brain mitochondrial function, brain metabolism, cerebral blood flow (CBF), and memory in young adult Surf1 KO mice.

MATERIALS AND METHODS

Animals

Male Surf1 KO mice[9] were generated from heterozygous crosses of Surf1$^{+/-}$ breeders in the C57/Bl6JxDBA2 background. Wild-type (WT) animals were littermates generated from the same crosses and served as controls. Mice were used at 6 to 7 months of age. All experiments were performed with approval by the IACUC (Institutional Animal Care and Use Committee) at the University of Texas Health Science Center at San Antonio.

Measures of Mitochondrial Function

Brain mitochondrial isolation. Whole brain mitochondria were isolated using differential centrifugation and Percoll gradients ($n = 6$ per experimental group). Because properties of somal mitochondria differ from synaptosomal mitochondria, a modification of the method by Zhou et al[10] was used to ensure separation of somal mitochondria from synaptosomes. All manipulations were performed at 4°C. Briefly, after CO_2 asphyxiation, brains were removed, then rinsed and minced in isolation buffer (250 mmol/L sucrose, 20 mmol/L Hepes, 1 mmol/L EDTA, 1 mmol/L EGTA, 1 mmol/L dithiothreitol) in the presence of $1 \times$ protease inhibitors (Cocktail set III; Calbiochem, San Diego, CA, USA). Brains were homogenized with a teflon pestle using 5 to 10 strokes and then centrifuged at $1,300 \times g$ for 10 minutes. The supernatant was collected, filtered through cheesecloth, and centrifuged again at $1,300 \times g$ for 10 minutes. The supernatant was then filtered through cheesecloth and centrifuged at $21,250 \times g$ for 10 minutes. The pellet was resuspended in 15% Percoll (GE Healthcare, Waukesha, WI, USA) in isolation buffer and spun at $65,400 \times g$ for 15 minutes. The supernatant was removed and the pellet was put on top of a preformed discontinuous Percoll gradient (23% and 40%) and spun at $65,400 \times g$ for 15 minutes. The mitochondrial fraction between the layers was collected, resuspended in isolation buffer, and spun at $65,400 \times g$ for 15 minutes. The pellet was resuspended again in isolation buffer plus 0.5% fatty acid-free bovine serum albumin and spun at $24,654 \times g$ for 10 minutes. The mitochondrial pellet was resuspended in isolation buffer and spun at $24,654 \times g$. The final pellet was resuspended in ROS buffer (125 mmol/L KCl, 10 mmol/L Hepes, 5 mmol/L $MgCl_2$, 2 mmol/L K_2HPO_4, pH 7.44) to be used in ATP production and oxygen consumption assays. Respiratory control ratios (state 3/state 4 respiration) were measured to evaluate mitochondria quality. Respiratory control ratio for brain mitochondria preparations was >9, indicating high-quality mitochondrial samples.

State 3 respiration. Mitochondrial oxygen consumption was measured using a Clark electrode (Oxytherm Oxygen Electrode Control Unit; Hansatech Instruments Ltd., Norfolk, UK) as described.[11] Briefly, mitochondria suspended in ROS buffer with 0.3% bovine serum albumin were used and glutamate (5 mmol/L)/malate (5 mmol/L) was the respiratory substrate.[12] State 3 respiration was induced with ADP (0.3 mmol/L).

ATP production. ATP production was measured in freshly isolated brain mitochondria using ATP Bioluminescence Assay Kit CLSII (Roche, Basel, Switzerland) and a fluorescent microplate reader. The substrates used were glutamate (2.5 mmol/L) and malate (2.5 mmol/L).[13]

Complex IV activity. Complex IV activity was measured by monitoring the oxidation of cytochrome C $2+$ at 550 nm using a spectrophotometer.[13] Mitochondria were prepared by suspending isolated brain mitochondria in ACA/BT buffer (750 mmol/L 6-aminocaprioic acid, 50 mmol/L Bis-Tris, pH 7.0) plus 1% n-dodecylmaltoside and $1 \times$ protease inhibitors (Cocktail set III) for 45 minutes with constant agitation at 4°C. The

suspension was then ultracentrifuged at $100,000 \times g$ for 15 minutes at 4°C. The protein concentration of the supernatant was measured using the Bradford method.[14] Preparation of reduced cytochrome c $(2+)$ was as follows: 500 μL of 8 mmol/L Cytochrome c $+3$ (Sigma, St Louis, MO, USA) was reduced with sodium borohydride (Sigma). To perform the Complex IV assay, 1 mL of the respiration buffer (250 mmol/L sucrose, 10 mmol/L KH_2PO_4, 1 mmol/L EGTA, 10 mmol/L Tris, pH 7.4) was placed into a polystyrene cuvette with 40 μmol/L cytochrome c $2+$. In all, 5 μg of mitochondrial protein was added, and the rate of cytochrome c $2+$ oxidation was measured at 550 nm.

Mitochondrial hydrogen peroxide production. Because hydrogen peroxide (H_2O_2) is a major contributor to oxidative damage, we used H_2O_2 as a measure of ROS production. The method we used was similar to that reported by Lustgarten et al.[15] Amplex red, which reacts with H_2O_2 in the presence of horseradish peroxidase to form resorufin, was used to assay H_2O_2 production in mitochondria isolated from brains. Resorufin fluorescence was measured at 544 nm excitation and 590 nm emission in a fluorescent microplate reader. Mitochondria were diluted in amplex red reagent buffer (amplex red 77.8 μmol/L, superoxide dismutase 37.5 units/mL, horseradish peroxidase 1 unit/mL in ROS buffer). Resorufin fluorescence was measured after the addition of glutamate (2.5 mmol/L) and malate (2.5 mmol/L). The H_2O_2 production was determined using an amplex red H_2O_2 standard curve.

Blood lactate levels. Blood lactate levels were measured in blood collected from the tail using a Lactate Plus lactate meter (Nova Biomedical, Waltham, MA, USA) as per the manufacturer's instructions.

In Vivo Neuroimaging

Animal preparation for functional neuroimaging. Six mice per experimental group were used in imaging studies. Animals that were used for functional imaging did not undergo behavioral testing, and their brain tissues were not used for biochemical determinations. Mice were anesthetized with 4.0% isoflurane for induction, and then maintained in a 1.2% isoflurane and air mixture using a face mask throughout the scans. Respiration rate (90 to 130 b.p.m.) and rectal temperature ($37 \pm 0.5^{\circ}$C) were continuously monitored. Heart rate and blood oxygen saturation level (SaO_2) were recorded using a MouseOx system (STARR Life Science Corp., Oakmont, PA, USA) and maintained within normal physiologic ranges.

Cerebral metabolic rate of glucose measurements. Mice were anesthetized under 1.2% isoflurane throughout the measurements. In all, 0.5 mCi of ^{18}FDG dissolved in 1 mL of physiologic saline solution was injected through the tail vein. Forty minutes were allowed for ^{18}FDG uptake before scanning. The animal was then moved to the scanner bed (Focus 220 MicroPET; Siemens, Nashville, TN, USA) and placed in the prone position. Emission data were acquired for 20 minutes in a three-dimensional list mode with intrinsic resolution of 1.5 mm. For image reconstruction, three-dimensional positron emission tomography (PET) data were rebinned into multiple frames of 1 second duration using a Fourier algorithm. After rebinning the data, a three-dimensional image was reconstructed for each frame using a 2D filtered back projection algorithm. Decay and dead time corrections were applied to the reconstruction process. Because ^{18}FDG is taken up by the whole body of the animal, we chose a 'region of interest' for our measurements that encompassed the whole brain, as outlined with a white line in Figure 2D, and determined cerebral metabolic rate of glucose (CMR_{Glc}) for whole brain using the mean standardized uptake value (SUV) equation: $SUV = (A \times W)/A_{inj}$, where A is the activity of the brain, W is the body weight of the mouse, and A_{inj} is the injection dose of ^{18}FDG.[16] We determined only *global* CMR_{Glc} because of the limited resolution of PET imaging (1.5 mm).

Cerebral blood flow measurements. Quantitative CBF (mL/g per minute) was measured using magnetic resonance imaging-based continuous arterial spin labeling techniques[17,18] on a horizontal 7T/30 cm magnet and a 40-G/cm BGA12S gradient insert (Bruker, Billerica, MA, USA). Mice were anesthetized under 1.2% isoflurane. A small circular surface coil (internal diameter = 1.1 cm) was placed on top of the head and a circular labeling coil (internal diameter = 0.8 cm), built into the cradle, was placed at the heart position for continuous arterial spin labeling. The two coils were positioned parallel to each other, separated by 2 cm from center to center, and were actively decoupled. Paired images were acquired in an interleaved manner with field of view = 12.8×12.8 mm^2,

matrix $= 128 \times 128$, slice thickness $= 1$ mm, 9 slices, labeling duration $= 2,100$ ms, repetition time $= 3,000$ ms, and echo time $= 20$ ms. Continuous arterial spin labeling image analysis used codes written in Matlab[17,18] and STIMULATE software (University of Minnesota, Minneapolis, MN, USA) to obtain CBF. The resolution (0.1 mm) allowed CBF to be determined both globally and regionally. Regional determinations in this study were performed in hippocampus and cortex because of their involvement in memory.

Brain metabolite determinations. [1]H magnetic resonance spectroscopy (MRS) was acquired with a point-resolved spectroscopy PRESS sequence. Animals were anesthetized under 1.2% isoflurane. A single voxel (3.5 mm cube) was placed at the isocenter of the mouse brain (water linewidth $= 17$ Hz) to determine the global concentration of brain metabolites. Parameters are repetition time/echo time $= 2,500/140$ ms; with (256 averages) and without (4 averages) VAPOR water suppression and outer volume suppression techniques. Data were processed using Bruker TOPSPIN software (TopSpin 2.1, Bruker BioSpin, Billerica, MA, USA), including Fourier transformation, magnitude calculation, frequency correction, phase correction, and baseline correction. Lactate (1.33 p.p.m.), N-acetyl aspartate (2.02 p.p.m.), creatine (Cr, 3.0 p.p.m.), and choline (Cho, 3.2 p.p.m.) concentrations were determined with the following equation:

$$[m] = \left(\frac{S_m}{S_r}\right)[r]C_n \qquad [1]$$

where $[m]$ is the concentration (in mmol/L) of the metabolite under investigation, S_m is the metabolite's signal from the spectra (with water suppression), S_r is the reference signal (water, obtained from the nonwater suppression measurement), $[r]$ is the concentration of the reference compound (55.14 mmol/L for water), and C_n is the correction for the number of equivalent nuclei for each resonance.

ATP concentrations. After completion of the ^{1}H MRS scans, the surface coil was tuned to [31]P Larmor frequency (121.6 MHz) and ^{31}P MRS was acquired with an NSPECT sequence. Parameters are repetition time $= 4,000$ ms and 160 averages. An additional measurement was performed with a 10-mmol/L phosphocreatine (PCr) phantom as the external reference. ATP concentration ([ATP]) in brain was determined by Equation (1), where with S_m is the ATP γ peak, S_r is the PCr peak from the phantom, and $[r]$ is the PCr concentration.

Behavioral Testing

Animals and conditions for behavioral testing. Ten mice per group were used for all tests. Animals that performed > 10 movements in the Y maze or did not engage in exploration of objects presented in the novel object recognition (NOR) task were excluded from the studies. Experiments were performed between 10:00 and 15:00 h. Whenever possible, animals were housed in groups with a maximum of four mice per cage. The same experimenter, blinded to genotype, performed all behavioral tests.

Y maze. We assessed working spatial memory in Surf1 KO mice and WT controls using the Y-maze task (see illustration in Figure 3A, left panel). Mice were placed at the middle of a Y-shaped maze and allowed to freely explore the three arms over an 8-minute period. The sequence and number of arm entries were recorded. The percentage of trials in which all three arms were represented was recorded as an alternation to estimate short-term memory of the last arms entered. The total number of possible alternations was calculated as the number of arm entries minus two. Unimpaired spatial working memory in rodents results in arm entry alternations at levels above chance. Total number of arm entries serve as a measure of spontaneous activity. Y maze tests were conducted in a standard procedure room with distinct features, which are expected to work as extramaze cues.

Novel object recognition. The NOR task was used to assess memory for interactions with novel objects. Animals tend to spend more time interacting with a new object rather than one they have previously encountered.[19] Experimental animals were habituated to the testing arena, a clean cage, 24 hours before training. On day 1, mice were presented with two different objects and allowed to explore them. On day 2, one of the objects was replaced with a new one (see illustration in Figure 3C). The amount of time mice spent exploring the novel and the previously encountered objects was recorded over 2 minutes. All objects were cleaned with 70% EtOH and allowed to completely dry between trials.

Elevated plus maze. Elevated plus maze (EPM) was used to assess basal anxiety levels, and to indirectly assess motivation. Mice were placed in the center of the maze and allowed to freely explore open and closed arms of the maze for 5 minutes. Mouse movements were recorded by a computer-based video tracking system (Maze2100; HVS Image, Mountain View, CA, USA). Activity levels were determined by measuring the total path length in the EPM, and the basal anxiety levels were determined by measuring the fraction of time spent in the closed arms of the EPM. Data were processed offline using HVS Image and then compiled with Microsoft Excel before statistical analyses.

Determinations of Protein Abundance

Western blotting. All biochemical determinations of relatively abundance of proteins of interest were performed using tissues from groups of mice that were neither used for behavioral testing, nor for functional imaging studies. Animals were euthanized by isoflurane overdose followed by cervical dislocation or by CO_2 inhalation. Brain tissues were obtained and homogenized in ice-cold homogenization buffer (50 mmol/L HEPES (pH 7.6), 150 mmol/L sodium chloride, 20 mmol/L sodium pyrophosphate, 20 mmol/L β-glycerophosphate, 10 mmol/L sodium fluoride, 2 mmol/L sodium orthovanadate, 2 mmol/L EDTA, 1.0% Igepal, 10% glycerol, 2 mmol/L phenylmethylsulfonyl fluoride, 1 mmol/L $MgCl_2$, 1 mmol/L $CaCl_2$, and protease inhibitor cocktail). The homogenates were kept on ice for 30 minutes and then centrifuged at $20,000 \times$ g. for 15 minutes. Protein concentrations in supernatants were determined using the Bradford method (Bio-Rad Laboratories, Hercules, CA, USA), which is linear with protein concentration in the ranges tested.[14] Equal amounts of total protein were loaded for all samples, resolved by sodium dodecyl sulfate-polyacrylamide gel electrophoresis, and transferred onto a nitrocellulose membrane. For HIF-1α immunoblots, membranes were stained with Ponceau-S before blocking to confirm equal loading. After blocking with 5% nonfat dry milk in Tris-buffered saline containing 0.1% Tween-20, the blots were probed with antibodies specific for P-CREB and CREB (Cell Signaling Technologies, Danvers, MA, USA) and HIF-1α (Cell Applications, San Diego, CA, USA). The membranes were then washed with Tris-buffered saline buffer with 0.5% Tween-20 and incubated with appropriate horseradish peroxidase-conjugated secondary antibodies (Santa Cruz Biotechnology, Santa Cruz, CA, USA). After washing with Tris-buffered saline buffer with 0.5% Tween-20, proteins were visualized by chemiluminescence using a Typhoon 8600 imager or by exposure to X-ray film (Kodak, Rochester, NY, USA). Densitometry was performed using Image Quant software (GE Healthcare) or NIH Image J (NIH, Bethesda, MD, USA). Total protein loaded in electrophoretic gels in all experiments were no saturating for the amounts of primary antibody used (antibody was in large excess). For all immunoblots, quantitations of optical density were performed in conditions of linearity for substrate oxidation by horseradish peroxidase (i.e., 4 to 5 minutes after initiation of the reaction). Light emission was measured within linear ranges either using multiple exposure times to X-ray film or by setting the Typhoon 8600 imager detector sensitivity such that no saturated pixels were present in the images in the conditions of the scans. Thus, as measured, optical densities were linear with oxidation of luminol to 3-aminophthalate by horseradish peroxidase for all proteins assayed.

Statistical Analyses

Statistical analyses were performed using GraphPad Prism (GraphPad, San Diego, CA, USA), Sigma Stat (Aspire Software International, Ashburn, VA, USA) or the R statistical language.[20] Significance of differences in means between two different groups was determined with Student's t-test, using t-test with Welch's correction when experimental samples did not show equal variances, or using a mixed-effect model[21] on scaled data for western blot experiments when different detection methods (i.e., imager scanning or exposure to X-ray film) were used in different individual experiments, such as in determinations of HIF-1α abundance. Because different imaging methods have different units and precisions, the data from each experiment were scaled by subtracting the experiment-wide mean and dividing by the experiment-wide standard error. A mixed-effect model[21] (R statistical language[20] with the name package[22]) was used to account for any other batch effects, where the scaled relative HIF-1α abundance was the response variable, genotype was the experimental variable, and membership in each experiment was the random variable. With this experimental design such a model gives results similar to a t-test, with a similar interpretation, but corrects for batch effects. Values of $P < 0.05$ were considered as significant.

RESULTS

Reduced Cytochrome C Oxidase Activity, Increased Hydrogen Peroxide Production, But Preserved ATP Levels in Mitochondria Isolated from Surf1 Knockout Mouse Brains

Mitochondria isolated from brains of Surf1 KO mice showed decreased COX activity ($-49 \pm 7\%$, $t = 6.45$, $df = 10$, $P < 0.001$; Figure 1A). They also had significantly increased H_2O_2 production[15] when glutamate/malate was used as the substrate ($24 \pm 10\%$, $t = 2.52$, $df = 9$, $P < 0.003$; Figure 1B). Consistent with decreased COX activity, State 3 (maximal) oxygen consumption was significantly decreased in Surf1 KO brain mitochondria ($-24 \pm 4\%$, $t = 2.56$, $df = 6$, $P < 0.05$; Figure 1C). However, despite the decrease in COX activity and respiration, there was only a small, nonsignificant decrease in ATP production (Figure 1D). In agreement with this observation, *in vivo* global ATP concentrations in brains of Surf1 KO mice measured with ^{31}P MRS were indistinguishable from those of WT mice (Figures 1E and 1F). Thus, Surf1 deficiency decreased COX activity and respiration without decreasing either ATP production in isolated mitochondria or ATP *in vivo* steady-state levels.

Increased Global Lactate Levels and Glucose Metabolism in Surf1 Knockout Mouse Brains

We next used proton ^{1}H MRS to determine lactate in brains of Surf1 KO and WT mice. Figure 2A shows representative ^{1}H spectra and Figure 2B shows global lactate concentrations determined from ^{1}H MRS. Surf1 KO mice showed significantly increased brain lactate concentrations ($37 \pm 7\%$, $t = 3.22$, $df = 10$, $P < 0.01$), but no changes in other brain metabolites such as N-acetyl aspartate (8.1 ± 1.5 versus 8.2 ± 1.7 mmol/L), creatine (5.6 ± 0.9 versus 5.5 ± 1.1 mmol/L), and choline (6.2 ± 0.8 versus 6.3 ± 0.9 mmol/L)

when compared with WT mice. Consistent with these data, we found significant increases in blood lactate concentrations in Surf1 KO mice relative to WT controls ($29 \pm 4\%$, $t = 1.88$, $df = 23$, $P < 0.05$, Figure 2C). To determine whether increased brain lactate in brains of Surf1 KO mice was accompanied by increased rates of brain glucose consumption, we measured CMR_{Glc} using PET in Surf1 KO and WT mice. Figure 2D shows representative CMR_{Glc} maps for the experimental groups. The color bar in Figure 2D depicts minimal and maximal linear values of CMR_{Glc}. Figure 2E shows quantitative analyses of CMR_{Glc} data. Surf1 KO mice had significantly increased global CMR_{Glc} ($38 \pm 9\%$, $t = 3.17$, $df = 10$, $P < 0.01$) relative to WT controls. Blood glucose levels in Surf1 KO mice under fed conditions were unchanged with respect to WT mice (8.86 ± 0.41 mmol/L for Surf1 KO versus 9.18 ± 0.44 mmol/L for WT), in agreement with previous reports that showed unchanged glucose levels in blood of Surf1 KO mice after a short-term (5-hour) or a long-term (16-hour) fast.[24]

Increased Global and Regional Cerebral Blood Flow in Surf1 Knockout Mouse Brains

Because increases in glucose metabolism can be accompanied by increases in cerebral perfusion,[25] we used magnetic resonance imaging to determine CBF in Surf1 KO and WT control mice. Single-slice CBF maps of WT and Surf1 KO mice (Figure 2F) include cortex and hippocampus, and correspond to the atlas images in Figures 2H and 2I. Figure 2G shows quantitative global CBF values for both experimental groups. Global CBF was increased in Surf1 KO mice with respect to WT mice ($32 \pm 6\%$, $t = 2.52$, $df = 10$, $P < 0.05$). Similarly, Surf1 KO mice showed increased cortical CBF ($37 \pm 8\%$ ($t = 3.48$, $df = 10$, $P < 0.01$, Figure 2H) and hippocampal CBF ($28 \pm 4\%$, $t = 3.43$, $df = 10$, $P < 0.01$, Figure 2I), compared with the WT mice. The differences in cortical CBF and hippocampal CBF between WT and Surf1 KO groups are illustrated by the single-slice CBF maps shown in Figure 2F.

Enhanced Working Spatial and Recognition Memory in Surf1 Knockout Mice

To determine whether the observed metabolic changes in Surf1KO mice were associated with changes in higher level processes, we assessed working spatial memory and recognition
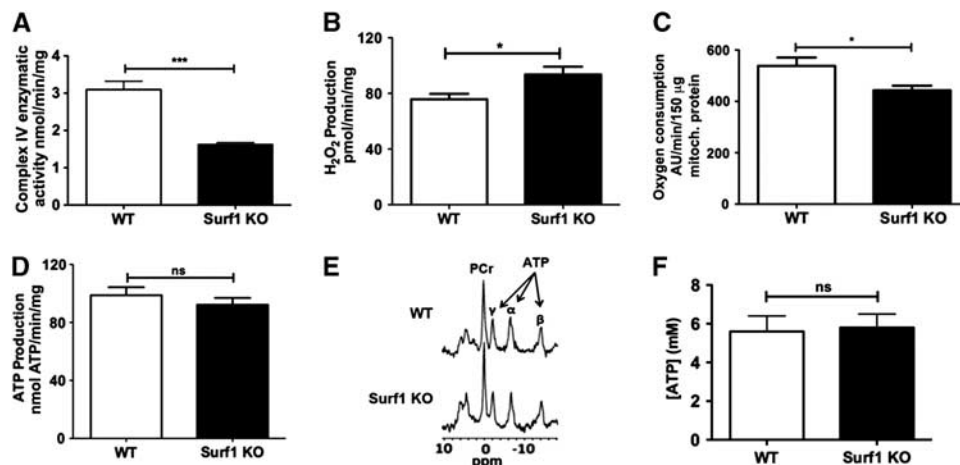

Figure 1. Lower cytochrome C oxidase (COX) activity and state 3 respiration with increased hydrogen peroxide (H_2O_2) generation, but preserved ATP levels, in mitochondria isolated from brains of Surf1 knockout (KO) mice. (**A**) Lower COX activity in mitochondria isolated from Surf1 KO as compared with wild-type (WT) mouse brains. (**B**) Higher H_2O_2 production in mitochondria from brains of Surf1 KO mice in response to complex 1-linked substrates (glutamate/malate). (**C**) Maximal mitochondrial respiration (state 3) was significantly decreased in mitochondria isolated from Surf1 KO as compared with WT mouse brains. (**D**) ATP production in response to complex 1-linked substrates (glutamate/malate) in isolated brain mitochondria was not significantly different between Surf1 KO and WT mice. $n = 5$ to 6 per experimental group. (**E**) ^{31}P magnetic resonance (MR) spectra, showing three peaks of ATP (α, β, γ) and creatine phosphate (PCr). (**F**) No significant differences were observed in ATP concentration in brains of Surf1 KO and WT mice as determined by ^{31}P MR spectroscopy (MRS). $n = 6$ per experimental group. Data are means $\pm$ s.e.m. *$P < 0.05$; ***$P < 0.001$, Student's *t*-test.
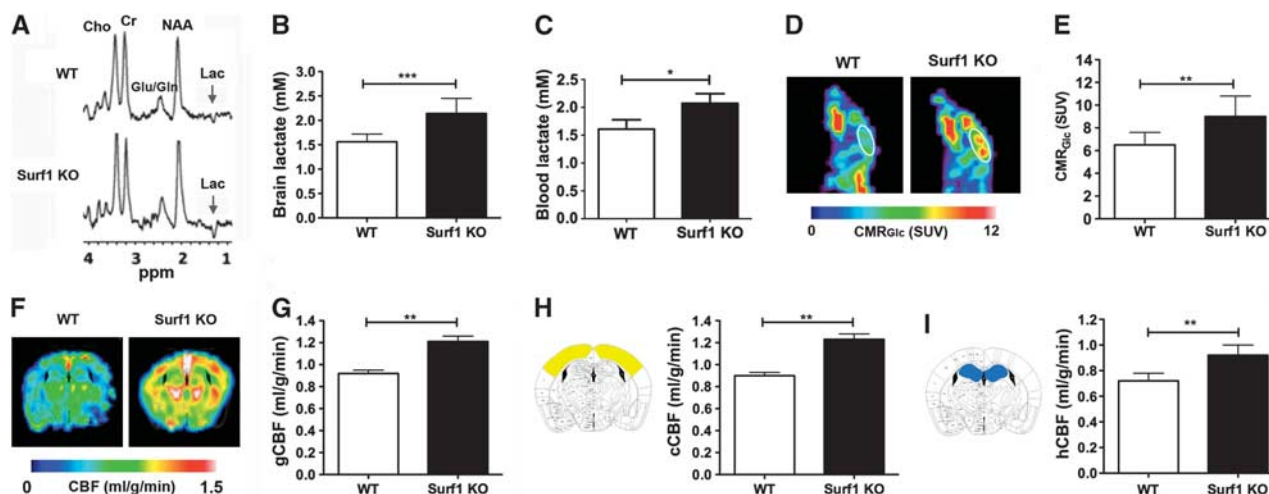
Figure 2. Increased lactate, cerebral metabolic rate of glucose (CMR$_{Glc}$), and cerebral blood flow (CBF) in Surf1 knockout (KO) brains. (**A**) Representative ^{1}H magnetic resonance (MR) spectra. (**B**) *In vivo* lactate concentration values [mmol/L] determined from ^{1}H magnetic resonance spectroscopy (MRS). (**C**) Blood lactate concentrations [mmol/L]. (**D**) CMR$_{Glc}$ maps of representative wild-type (WT) and Surf1 KO mice obtained by positron emission tomography (PET). The white line indicates the whole brain, which was considered as region of interest 'ROI'. (**E**) CMR$_{Glc}$ as standardized uptake values (SUVs). (**F**) Representative CBF maps of WT and Surf1 KO mice obtained by magnetic resonance imaging (MRI). (**G**) Global CBF (gCBF) (mL/g per minute) for Surf1 KO and WT mice. (**H**) Cortical CBF values (cCBF, right panel) and brain atlas image showing cortical regions included in the measurements (left panel). (**I**) Hippocampal CBF (hCBF, right panel) and brain atlas image showing hippocampal regions included in the measurements (left panel). $n = 6$ per experimental group. The color scales for CMR$_{Glc}$ and CBF are linear. The demarcations show minimal and maximal values in the linear scale. Data are means ± s.e.m. *$P < 0.05$; **$P < 0.01$; ***$P < 0.001$, Student's t-test. Lac, lactate; Cr, creatine; Cho, choline; NAA, N-acetyl aspartate; Glu/Gln, glutamate/glutamine.

memory in Surf1 KO and WT mice using the Y maze and the NOR tasks. Surf1 KO mice showed significantly increased alternations in the Y maze compared with the WT group ($38 \pm 8\%$, $t = 2.69$, df $= 15$, $P < 0.05$, Figure 3A). Surf1 KO mice also spent more time exploring a novel object in the NOR task relative to WT animals ($46 \pm 10\%$, $t = 2.32$, df $= 8$, $P < 0.05$, t-test with Welch's correction, Figure 3C). These results indicate that Surf1 KO mice have enhanced working spatial and recognition memory. Because cognitive outcomes can be strongly influenced by noncognitive components of behavior, we measured basal anxiety using the EPM. No differences were observed in the fraction of time spent in the closed arms (Figure 3D), nor in total path length (Figure 3E) in the EPM, indicating similar basal anxiety and activity levels, respectively, in Surf1 KO and WT mice. In agreement with their similar levels of basal activity levels in the EPM, total arm entries in the Y maze were indistinguishable in WT and Surf1 KO animals (Figure 3B). Taken together, these results suggest that Surf1 deficiency enhances spatial and recognition memory but does not affect basal anxiety levels nor activity, ruling out a role of anxiety and motivation in the enhanced performance of Surf1 KO mice in tasks testing working and recognition memory.

Increased Hypoxia-Inducible Factor 1 Alpha and Phosphorylated Cyclic AMP Response Element-Binding in Surf1 Knockout Mouse Brains

Cytochrome C oxidase deficiency induced increased H$_2$O$_2$ production in mitochondria isolated from Surf1 KO brains (Figure 1B). Because increases in ROS have been shown to stabilize HIF-1α,[3,26] we hypothesized that HIF-1α[3,26] may be increased in brains of Surf1 KO mice. To test this hypothesis, we examined HIF-1α levels in brains of Surf1 KO mice and WT control littermates. Levels of HIF-1α in Surf1 KO mouse brain lysates were increased by $50 \pm 10\%$ compared with WT brains (Figures 3F and 3G, $t = 2.63$, df $= 17$, $P < 0.01$). The abundance of HIF-1α in Surf1 KO samples was approximately one standard deviation greater than that of WT samples (1.002, $t = 2.63$, df $= 17$, $P = 0.01$). HIF-1α can stabilize and

activate its coactivator CREB,[7] which is critically involved in the processes thought to underlie the formation of long-term memory.[8] Similar to the effect observed for HIF-1α abundance, brains of Surf1 KO mice had significantly increased levels of phosphorylated (activated) CREB (pCREB; $25 \pm 6\%$, $t = 3.01$, df $= 10$, $P < 0.01$) as compared with WT animals (Figures 3H and 3I).

DISCUSSION

Our data show that long-lived[9] Surf1 KO mice have significantly enhanced CMR$_{Glc}$, increased CBF, increased brain lactate, and increased levels of HIF-1α and pCREB, as well as enhanced working and recognition memory. ATP production in brain mitochondria isolated from Surf1 KO mice remained unchanged despite a 49% reduction in COX activity, a 24% reduction in state 3 respiration, and a 24% increase in H$_2$O$_2$ production. ATP levels were also unchanged in Surf1-deficient brains.

In agreement with prior studies,[9] blood lactate in Surf1 KO mice was higher than in WT mice, indicating a partial block in the aerobic metabolism of pyruvate in peripheral tissues.[9] Alterations in peripheral glucose metabolism may lead to changes in blood glucose levels, which could in turn alter the rates of transport and metabolism of ^{18}F-FDG. Blood glucose levels in Surf1 KO mice, however, were not changed under fed conditions (in our studies) nor after short-term or long-term fasting in the studies of Deepa et al,[24] ruling out this potential confound in the semiquantitative assessment of CMR$_{Glc}$.

The increase in CMR$_{Glc}$ in Surf1 KO brains indicates a moderate increase in brain glucose utilization. Lactate levels were also moderately increased in Surf1-deficient brains. Maintained ATP levels, however, argue against a significant block in respiration rates in Surf1 KO brains because of excess capacity of COX *in vivo*.[27,28] Moreover, because blood lactate is increased in Surf1 KO animals, it is possible that elevated brain lactate levels result from concentration-driven transport of lactate from blood. Additional studies including direct measurements of *in vivo* respiration
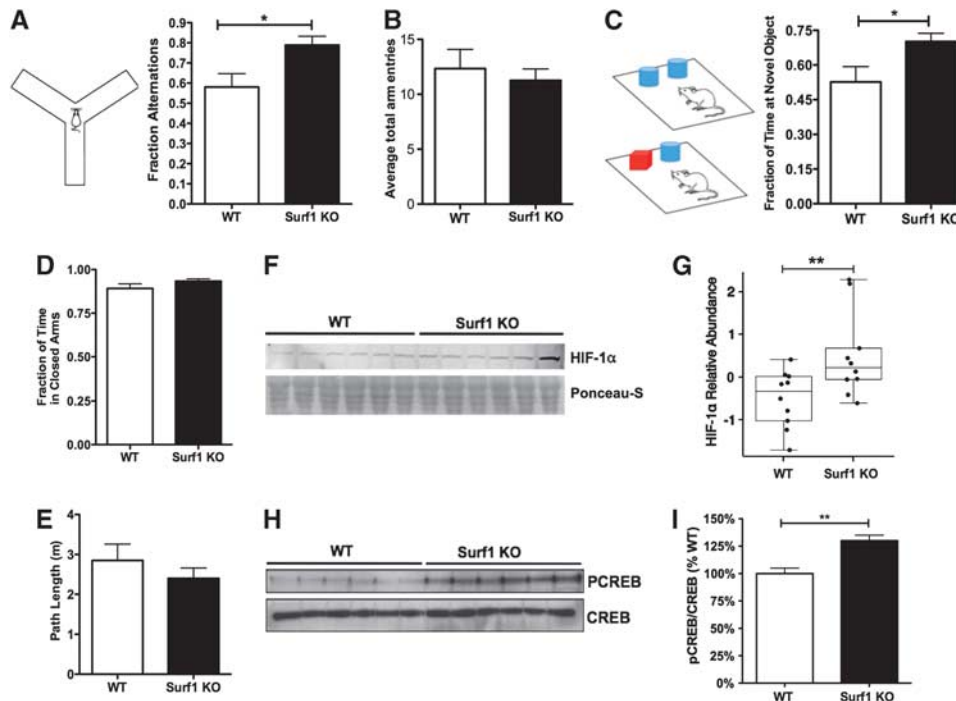
Figure 3. Enhanced memory and increased hypoxia-inducible factor 1 alpha (HIF-1α) and phosphorylated cyclic AMP response element binding (pCREB) in Surf1 knockout (KO) mice. (**A, B**) Enhanced working memory, as measured by increased arm alternations (**A**, right panel) during exploration of a Y-shaped maze (**A**, left panel), but no difference in total arm entries (as a measure of basal activity, **B**) in Surf KO as compared with wild-type (WT) mice. (**C**) Enhanced memory of a previously encountered object, measured by increased time exploring a novel object (right panel) in Surf1 KO as compared with WT mice. (**D**) Basal anxiety, measured as fraction of time spent in the closed arms of an elevated maze, was not different between Surf1 KO and WT control mice. (**E**) Basal activity levels, as total distance traveled in the elevated maze, were not different between experimental groups. $n = 5$ to 10 per experimental group. (**F**) Top panel, representative immunoblot of brain extracts from WT and Surf1 KO mice probed with antibodies specific for HIF-1α; lower panel, membrane shown in (**A**) stained with Ponceau-S, showing comparable total protein loading for all samples. (**G**) Quantitative analyses of HIF-1α immunoreactivity in brain lysates from Surf1 KO and WT mice. (**H**) Representative immunoblots of brain extracts from WT and Surf1 KO mice probed with antibodies specific for phospho-CREB(Ser133) (P-CREB) and CREB. (**I**) Quantitative analyses of P-CREB/CREB immunoreactivity in brain lysates from Surf1 KO and WT mice. $n = 10$ per experimental group. Data are means ± s.e.m. *$P < 0.05$; **$P < 0.01$, Student's *t*-test except for (**E**), where significance of differences was determined using a mixed-effect model as in Materials and methods.

rates are needed to determine the precise interactions between different metabolic pathways in Surf1-deficient brains.

Even though we cannot infer changes in H_2O_2 levels *in vivo* from the observed *in vitro* increases in H_2O_2 production in mitochondria isolated from Surf1 KO brains, it is possible that even mild increases in H_2O_2 in brains from Surf1-deficient mice may lead to the stabilization of HIF-1α.[3,26] HIF-1α, in turn, can stabilize and activate its coactivator CREB,[7] which is critically involved in the processes believed to underlie the formation of long-term memory.[8] In agreement with the observed increases in brain HIF-1α, we found that activated CREB was increased and recognition memory was enhanced in Surf1 KO mice. The increases in CBF in brain regions related to memory (i.e., cortex and hippocampus) could thus be driven by increased CMR_{Glc} associated with enhanced functional activation. Hence, increased HIF-1α signaling may influence processes of memory formation in Surf1 KO mice.

The findings of this study are consistent with prior evidence from invertebrate models, suggesting that decreased mitochondrial respiration and increased ROS generation could have beneficial effects.[3,4] Although it is well documented that exceedingly increased ROS can damage cellular structure/function and thus accelerate aging and shorten lifespan,[1] emerging evidence shows that *mild* increases in ROS (such as those arising from partial inhibition of mitochondrial respiration) may cause opposite effects, including increases in lifespan and

protection against age-related disease.[3,4,29] Mild increases of ROS formation in mitochondria may cause an adaptive response (dubbed 'mitohormesis'; Ristow and Zarsek[29] and Schulz et al[30]) that leads to increased stress resistance, believed to ultimately cause a long-term reduction in oxidative stress.[29]

Taken together, our data indicate that Surf1-induced mitochondrial dysfunction could lead to physiologic adaptations that ultimately result in enhanced neuroprotection[9] and enhanced cognitive function. In agreement with this hypothesis, mice in which Coq7, a mitochondrial hydroxylase necessary for the synthesis of ubiquinone, is reduced by half (Mclk1$^{+/-}$ mice) have enhanced resistance to neurologic damage.[31] Mitochondrial dysfunction arising from Surf1 deficiency, however, may not be beneficial in all tissue systems. Despite enhanced brain functionality, we observed impairments associated with swimming in Surf1 KO mice. This deficiency was severe enough to preclude some behavioral tests such as the Morris water maze, which require unencumbered swimming.

Another limitation of the present study is that we used isoflurane to anesthetize the animals during functional imaging experiments. This intervention may have lowered brain metabolism; and thus our measurements may not be representative of brain metabolism in the conscious state.[32] In addition, isoflurane anesthesia may, itself, disturb the tissue's metabolic profile, such as by increasing lactate, as compared with propofol anesthesia.[33] To minimize these potential confounds, we used low

concentrations of isoflurane for anesthesia and monitored respiration rates and rectal temperatures continuously for all experimental groups during functional imaging experiments. Although we cannot rule out a potential effect of isoflurane in our results, at the dose used, isoflurane anesthesia did not affect basic physiologic parameters for animals of either genotype while measurements were taken. Furthermore, and supporting the notion that our in vivo measurements of brain lactate concentration in WT and Surf1 KO mice were not grossly affected by isoflurane anesthesia, blood lactate levels in conscious Surf1 KO animals were consistent with and showed the same direction of change as brain lactate levels measured in vivo. Thus, it is unlikely that the differences in brain lactate levels between WT and Surf1 KO measured with in vivo brain imaging are due to differential effects of isoflurane anesthesia in Surf1 KO and WT mice.

In conclusion, the present studies show that reduced oxygen consumption and increased H_2O_2 generation without changes in ATP production by Surf1-deficient brain mitochondria in vitro are associated with maintained brain ATP levels, increased glucose metabolism, increased CBF, and enhanced working and recognition memory in vivo in Surf1 KO mice. Future studies assessing the relationship between in vivo mitochondrial function, ROS generation, and brain functionality will have important implications for our understanding of cognitive aging and age-related neurologic disorders.

DISCLOSURE/CONFLICT OF INTEREST
The authors declare no conflict of interest.

REFERENCES
1 Harman D. Free radical theory of aging: dietary implications. Am J Clin Nutr 1972; 25: 839–843.
2 Kirchman PA, Kim S, Lai CY, Jazwinski SM. Interorganelle signaling is a determinant of longevity in Saccharomyces cerevisiae. Genetics 1999; 152: 179–190.
3 Lee SJ, Hwang AB, Kenyon C. Inhibition of respiration extends C. elegans life span via reactive oxygen species that increase HIF-1 activity. Curr Biol 2010; 20: 2131–2136.
4 Rea SL, Ventura N, Johnson TE. Relationship between mitochondrial electron transport chain dysfunction, development, and life extension in Caenorhabditis elegans. PLoS Biol 2007; 5: e259.
5 Yang W, Hekimi S. Two modes of mitochondrial dysfunction lead independently to lifespan extension in Caenorhabditis elegans. Aging Cell 2010; 9: 433–447.
6 Kallio PJ, Wilson WJ, O'Brien S, Makino Y, Poellinger L. Regulation of the hypoxia-inducible transcription factor 1alpha by the ubiquitin-proteasome pathway. J Biol Chem 1999; 274: 6519–6525.
7 Carrero P, Okamoto K, Coumailleau P, O'Brien S, Tanaka H, Poellinger L. Redox-regulated recruitment of the transcriptional coactivators CREB-binding protein and SRC-1 to hypoxia-inducible factor 1alpha. Mol Cell Biol 2000; 20: 402–415.
8 Viola H, Furman M, Izquierdo LA, Alonso M, Barros DM, de Souza MM et al. Phosphorylated cAMP response element-binding protein as a molecular marker of memory processing in rat hippocampus: effect of novelty. J Neurosci 2000; 20: RC112.
9 Dell'agnello C, Leo S, Agostino A, Szabadkai G, Tiveron C, Zulian A et al. Increased longevity and refractoriness to Ca(2+)-dependent neurodegeneration in Surf1 knockout mice. Hum Mol Genet 2007; 16: 431–444.
10 Zhou Q, Lam PY, Han D, Cadenas E. c-Jun N-terminal kinase regulates mitochondrial bioenergetics by modulating pyruvate dehydrogenase activity in primary cortical neurons. J Neurochem 2008; 104: 325–335.
11 Hinkle PC. P/O ratios of mitochondrial oxidative phosphorylation. Biochim Biophys Acta 2005; 1706: 1–11.
12 Hynes J, Marroquin LD, Ogurtsov VI, Christiansen KN, Stevens GJ, Papkovsky DB et al. Investigation of drug-induced mitochondrial toxicity using fluorescence-based oxygen-sensitive probes. Toxicol Sci 2006; 92: 186–200.
13 Shi Y, Pulliam DA, Liu Y, Hamilton RT, Jernigan AL, Bhattacharya A et al. Reduced mitochondrial ROS, enhanced antioxidant defense, and distinct age-related changes in oxidative damage in muscles of long-lived Peromyscus leucopus. Am J Physiol Regul Integr Comp Physiol 2013; 304: R343–R355.
14 Zor T, Selinger Z. Linearization of the Bradford protein assay increases its sensitivity: theoretical and experimental studies. Anal Biochem 1996; 236: 302–308.
15 Lustgarten MS, Jang YC, Liu Y, Muller FL, Qi W, Steinhelper M et al. Conditional knockout of Mn-SOD targeted to type IIB skeletal muscle fibers increases oxidative stress and is sufficient to alter aerobic exercise capacity. Am J Physiol Cell Physiol 2009; 297: C1520–C1532.
16 Lee WC, Chang CH, Ho CL, Chen LC, Wu YH, Chen JT et al. Early detection of tumor response by FLT/microPET Imaging in a C26 murine colon carcinoma solid tumor animal model. J Biomed Biotechnol 2011; 2011: 535902.
17 Muir ER, Shen Q, Duong TQ. Cerebral blood flow MRI in mice using the cardiac-spin-labeling technique. Magn Reson Med 2008; 60: 744–748.
18 Duong TQ, Silva AC, Lee SP, Kim SG. Functional MRI of calcium-dependent synaptic activity: cross correlation with CBF and BOLD measurements. Magn Reson Med 2000; 43: 383–392.
19 Antunes M, Biala G. The novel object recognition memory: neurobiology, test procedure, and its modifications. Cogn Process 2012; 13: 93–110.
20 Team RDC (eds) R: A Language and Environment for Statistical Computing. R Foundation for Statistical Computing: Vienna, Austria, 2011.
21 Pinheiro J, Bates D. Mixed-Effects Models in S and S-PLUS. Springer: New York, NY, 2000.
22 Pinheiro J, Bates D, DebRoy S, Sarkar D, Team RDC. nlme: Linear and Nonlinear Mixed Effects Models. http://cran.r-project.org/web/packages/nlme/nlme.pdf.
23 Kilkenny C, Browne WJ, Cuthill IC, Emerson M, Altman DG. Improving bioscience research reporting: the ARRIVE guidelines for reporting animal research. PLoS Biol 2010; 8: e1000412.
24 Deepa SS, Pulliam D, Hill S, Shi Y, Walsh ME, Salmon A et al. Improved insulin sensitivity associated with reduced mitochondrial complex IV assembly and activity. FASEB J 2013; 27: 1371–1380.
25 Fox PT, Raichle ME, Mintun MA, Dence C. Nonoxidative glucose consumption during focal physiologic neural activity. Science 1988; 241: 462–464.
26 Xie M, Roy R. Increased levels of hydrogen peroxide induce a HIF-1-dependent modification of lipid metabolism in AMPK compromised C. elegans dauer larvae. Cell Metab 2012; 16: 322–335.
27 Katsura K, Folbergrova J, Gido G, Siesjo BK. Functional, metabolic, and circulatory changes associated with seizure activity in the postischemic brain. J Neurochem 1994; 62: 1511–1515.
28 Meldrum BS, Nilsson B. Cerebral blood flow and metabolic rate early and late in prolonged epileptic seizures induced in rats by bicuculline. Brain 1976; 99: 523–542.
29 Ristow M, Zarse K. How increased oxidative stress promotes longevity and metabolic health: The concept of mitochondrial hormesis (mitohormesis). Exp Gerontol 2010; 45: 410–418.
30 Schulz TJ, Zarse K, Voigt A, Urban N, Birringer M, Ristow M. Glucose restriction extends Caenorhabditis elegans life span by inducing mitochondrial respiration and increasing oxidative stress. Cell Metab 2007; 6: 280–293.
31 Zheng H, Lapointe J, Hekimi S. Lifelong protection from global cerebral ischemia and reperfusion in long-lived Mclk1(+/)(−) mutants. Exp Neurol 2010; 223: 557–565.
32 Alkire MT, Pomfrett CJ, Haier RJ, Gianzero MV, Chan CM, Jacobsen BP et al. Functional brain imaging during anesthesia in humans: effects of halothane on global and regional cerebral glucose metabolism. Anesthesiology 1999; 90: 701–709.
33 Makaryus R, Lee H, Yu M, Zhang S, Smith SD, Rebecchi M et al. The metabolomic profile during isoflurane anesthesia differs from propofol anesthesia in the live rodent brain. J Cereb Blood Flow Metab 2011; 31: 1432–1442.